We are IntechOpen, the world's leading publisher of Open Access books
Built by scientists, for scientists

4,400
Open access books available

117,000
International authors and editors

130M
Downloads

Our authors are among the

154
Countries delivered to

TOP 1%
most cited scientists

12.2%
Contributors from top 500 universities

CLARIVATE ANALYTICS
BOOK CITATION INDEX
INDEXED

WEB OF SCIENCE™

Selection of our books indexed in the Book Citation Index in Web of Science™ Core Collection (BKCI)

Interested in publishing with us?
Contact book.department@intechopen.com

Numbers displayed above are based on latest data collected.
For more information visit www.intechopen.com

15

Molecular Imaging of Breast Cancer Tissue *via* Site-Directed Radiopharmaceuticals

Andrew B. Jackson, Lauren B. Retzloff,
Prasant K. Nanda and C. Jeffrey Smith
University of Missouri Department of Radiology, Columbia, MO
United States of America

1. Introduction

The American Cancer Society reports that ~261,100 new cases of invasive and in situ breast cancer were diagnosed in 2010, and nearly 40,000 fatalities were attributed to this disease (American Cancer Society, 2010). Although death rates have steadily decreased since 1990, breast cancer currently ranks second in cancer deaths among women. Improvements in detection, treatment, and prevention education contribute to slow the incidence rate, and rapidly evolving nuclear medicine techniques have emerged as a formidable opponent to female breast cancer. The involvement of nuclear medicine imaging modalities in both the detection and diagnosis of breast cancer has increased in recent years (Gopalan et al., 2002). In contrast to earlier imaging methods, in which the transmission of various forms of energy through tissue is employed to generate an image, nuclear medicine imaging techniques are based on detection of the energy emitted from radioactive tracers that are injected into the body and subsequently accumulate locally in specific tissues (Nass et al., 2001). The classification of these techniques as either positron emission tomography (PET) or single photon emission computed tomography (SPECT) imaging modalities is determined by the radionuclide that is utilized to synthesize a given radiotracer.

The theory behind nuclear medicine imaging techniques to detect and diagnose breast cancer is founded on preferential radiopharmaceutical uptake by cancerous cells as a result of alterations in metabolic rate, vascularity, or receptor expression which are associated with malignancy. Although both PET and SPECT are commonly employed to detect a variety of malignancies, neither imaging technique has achieved clinical acceptance as a method of imaging breast cancer due to the lack of sensitivity and specificity demonstrated by available radiotracers (Gopalan et al., 2002; Nass et al., 2001; Rosen et al., 2008).

Presently, there is only one radiopharmaceutical, the SPECT imaging agent technetium-99m methoxy-isobutyl-isonitrile (^{99m}Tc-sestamibi, Miraluma®), that has received FDA approval for use as a diagnostic adjunct to mammography (Gopalan et al., 2002; Nass et al., 2001; Rosen et al., 2008). Although the mechanism governing the concentration of ^{99m}Tc-sestamibi in cancer cells is not fully understood, it may be related to the degree of cellular proliferation and vascular permeability (Nass et al., 2001). Once inside malignant cells, ^{99m}Tc-sestamibi is

sequestered within the cytoplasm as a result of the strong electrostatic attraction between the positively charged lipophilic ^{99m}Tc-sestamibi and the negatively charged mitochondria. This sequestration allows for the accumulation of ^{99m}Tc-sestamibi in cancer cells over time, presenting with high contrast on the resulting SPECT image (Gopalan et al., 2002). Despite the relatively high overall sensitivity (75-95%), specificity (71-100%), positive predictive value (67-100%), and accuracy (67-92%) demonstrated in numerous trials, ^{99m}Tc-sestamibi has proven unsuitable for the diagnosis of lesions smaller than 12 millimeters due to a significant decrease in both sensitivity (30-50%) and specificity (50%) (Gopalan et al., 2002).

2. Current research: Toward receptor-targeted radiopharmaceuticals

The continued interest in the development of radiopharmaceuticals for the detection and diagnosis of breast cancer is based on the fact that current methods fail to both detect and accurately diagnose early stage lesions in a large percentage of patients (Berghammer et al., 2001; Gopalan et al., 2002; Olsen & Gotzsche 2001). Nuclear medicine imaging techniques are well suited to address this situation given their ability to noninvasively detect a variety of physiological alterations associated with malignancy. The potential clinical applications of scintigraphic evaluation of breast cancer patients fall into five categories: 1) the early detection of breast cancer, 2) the differentiation between benign and malignant masses, 3) the staging of newly discovered breast cancer, 4) the detection of distant metastatic sites, and 5) the evaluation of tumor response to therapy (Berghammer et al., 2001; Rosen et al., 2008).

2.1 Early radiopharmaceuticals

While radiolabeled small molecules have accounted for the vast majority of imaging agents initially investigated for breast cancer detection and diagnosis, their non-specificity has resulted in low accumulation in target tissues, high levels of background radioactivity, and poor image resolution (Anderson & Welch, 1999). As a consequence of these findings, research efforts have shifted towards the utilization of monoclonal antibodies, which have been designed to target specific antigens that are over-expressed on tumor cells (Signore et al., 2001).

However, radiolabeled monoclonal antibodies have had limited clinical success due to several factors including the immunogenicity of the murine antibodies frequently employed in radiotracer preparation, the predominately hepatobiliary route of excretion, and the reduced ability to extravasate and access the target antigen as a result of the large size of intact monoclonal antibodies (Blok et al., 1999).Although the introduction of Fab´ and $F(ab)_2$´ fragments, chimeric, and humanized antibodies have diminished these effects, accumulation of monoclonal antibodies in tumor tissue continues to be insufficient, generating unfavorable target to background ratios.The advent of radiolabeled biologically active peptides in the early 1990s provided a means to overcome the limitations associated with these early radiopharmaceuticals (Table 1) (Fischman et al., 1993).The unique over-expression of specific receptors on malignant cells allows for their selective targeting using radiolabeled peptides that are designed to act as ligands for these receptors (Katzenellenbogen et al., 1995). A number of these receptor targets that are described herein

have been identified on breast cancer cells, including those for somatostatin, vasoactive intestinal peptide, neuropeptide Y, and gastrin releasing peptide.

	Small Molecules	**Monoclonal Antibodies**	**Peptides**
Synthesis	Facile	Lengthy	Facile
Size	Less than 1,500Da	MAb: ~160kDa, Fab´ and $F(ab)_2$´ Fragments: 10-100kDa	Less than 10,000Da
Specificity	Moderate	High, Inflammation Sites: Nonspecific IgG uptake	High
Binding Affinity	Perfusion Agents: N/A, Others: Moderate	High	High
***In Vivo* Binding**	Perfusion Agents: N/A, Others: Moderate	Limited by size	High
Target to Background Ratio	Moderate	Moderate	Moderate to High
Blood Clearance	Variable	Slow	Rapid
Immunogenicity	No	Potential for HAMA response	No

Table 1. Comparison of Early Radiopharmaceuticals (Blok et al., 1999; Fischman et al., 1993; Signore et al., 2001)

2.2 Somatostatin receptor scintigraphy

Somatostatin (SST) is a peptide hormone with two endogenous forms, SST-14 and SST-28, which are the cleavage products of the SST prohormone. SST may be found in several organ systems, including the central nervous system, the hypothalamopituitary system, the gastrointestinal tract, the exocrine and endocrine pancreas, and the immune system. This widespread distribution highlights the varied actions of SST throughout the body, ranging from inhibition of peptide hormone secretion to modulation of neurotransmission to inhibition of cellular proliferation. These effects are mediated *via* interaction with G protein-coupled SST receptors, which may lead to a number of intracellular actions including the inhibition of the adenylyl cyclase-cAMP-protein kinase A and MAP kinase (MAPK) pathways, modulation of potassium channels, stimulation of phopholipase A2, and activation of phosphotyrosine phosphatases. To date, five SST receptor subtypes have been identified ($SSTR_1$, $SSTR_2$, $SSTR_3$, $SSTR_4$, $SSTR_5$), which differ in both their expression pattern and their affinity for structural analogs of SST (Pomper & Gelovani, 2008; Reubi, 2008).

The observation that the administration of SST inhibits the growth of various tumor cell lines as a result of their over-expression of the SST receptor led to the development of OctreoScan® (^{111}In-diethylenetriaminepentaacetic acid (DTPA)-octreotide), a radiolabeled synthetic SST analog that became the first peptide-based radiopharmaceutical to receive FDA approval for the scintigraphic localization of SST receptor-positive neuroendocrine tumors. Due to the fact that endogenous SST exhibits a short *in vivo* half-life as a result of

rapid degradation by both aminopeptidases and endopeptidases, OctreoScan® incorporates modified amino acids into the Phe-(D)Trp-Lys-Thr receptor binding motif of octreotide to inhibit its metabolism and allow for increased tumor uptake.

The discovery that SST receptors are expressed on a multitude of tumor types, including those of the breast (50-75%), coupled with the diagnostic and therapeutic success of OctreoScan® in patients with neuroendocrine carcinomas, generated interest in the potential expansion of OctreoScan®'s clinical use. While the successful scintigraphic detection of both primary and metastatic breast cancer has been reported with OctreoScan® in 50 to 94% of breast cancer cases, these figures may represent an overestimation as nonspecific uptake by nonmalignant breast tissue is observed in 15% of patients (Bajc et al., 1996; Reubi, 2008; Wang et al., 2008). In addition to the nonspecific uptake observed with OctreoScan®, the low density of SST receptors ($SSTR_{2A}$ and $SSTR_5$) present in carcinomas of the breast combined with their heterogeneous expression pattern have prevented the acceptance of this agent for the routine diagnosis of breast cancer.

2.3 Vasoactive intestinal peptide scintigraphy

Vasoactive intestinal peptide (VIP) is a neuropeptide composed of 28 amino acids that belongs to the glucagon secretion family of peptides. VIP, and the closely related pituitary adenylate cyclase-activating polypeptide (PACAP), are among the most important neurotransmitters employed in the digestive system. In addition to its actions in the gut, VIP has a modulatory role in both the central nervous and immune systems. These actions are mediated by binding to G protein-coupled VIP receptors ($VPAC_1$, $VPAC_2$), which may be internalized after ligand binding, resulting in various intracellular effects including stimulation of adenylyl cyclase activity (Pomper & Gelovani, 2008; Reubi, 2008). The $VPAC_1$ and $VPAC_2$ receptors exhibit distinct distribution patterns, with preferential expression of the $VPAC_1$ receptor in a number of tissues including hepatocytes, gastrointestinal mucosa, pancreatic ducts, lung acini, thyroid follicles, prostatic glands, bladder and ureter urothelium, and breast lobules and ducts and of the $VPAC_2$ receptor in smooth muscle. In addition to its ubiquitous *in vivo* biodistribution pattern, the $VPAC_1$ receptor has been reported to be expressed in up to 93% of all primary tumors and metastatic sites of lung and breast cancer, generating interest in the development of $VPAC_1$-targeted radiotracers that may be employed in the detection and diagnosis of various neoplasms (Moody & Gozes, 2007; Pomper & Gelovani, 2008; Reubi, 2008).

Radiopharmacological targeting of the $VPAC_1$ receptor in colon cancer tumors was initially accomplished by radiolabeling native VIP with iodine-123 (^{123}I). While promising scintigraphic images have been obtained using this agent, the rapid *in vivo* degradation of endogenous VIP, combined with both the cost and the difficulty associated with ^{123}I-VIP conjugate synthesis, have hindered widespread clinical use of this compound. In an effort to address these issues, investigators have constructed a variety of VIP analogs that are suitable for labeling with a number of radioisotopes including technetium-99m (^{99m}Tc), copper-64 (^{64}Cu), and fluorine-18 (^{18}F) (Moody & Gozes, 2007; Pomper & Gelovani, 2008; Thakur et al., 2004). Although these radiotracers have proven capable of *in vivo* targeting of $VPAC_1$ receptor-bearing tumors, the significant background radioactivity that is present as a result of ubiquitous $VPAC_1$ receptor expression and the rapid *in vivo* degradation of these VIP analogs reduces the resolution of the images obtained. These results, coupled with the fact that $VPAC_1$ receptors are found in high (>2,000 dpm/mg tissue) density in only 37% of

breast tumors, suggest that radiolabeled VIP conjugates are unlikely to gain widespread clinical acceptance for use in routine breast cancer detection and diagnosis.

2.4 Neuropeptide Y receptor scintigraphy

Neuropeptide Y (NPY) is a neurotransmitter that belongs to a family of 36 amino-acid-long peptides that also includes peptide YY and pancreatic polypeptide. In the central nervous system, the actions of NPY consist of stimulation of feeding behavior and inhibition of anxiety, while in the peripheral nervous system NPY regulates a variety of functions such as vasoconstriction, gastrointestinal motility and secretion, insulin release, and renal function (Koglin & Beck-Sickinger, 2004; Reubi, 2008). These effects are mediated by interaction with various metabotropic G protein-coupled NPY receptor subtypes (Y_1, Y_2, Y_3, Y_4, Y_5, Y_6), among which Y_1, Y_2, Y_4, and Y_5 have been well characterized.

In contrast to other regulatory peptides, NPY has not often been associated with human cancer. However, a recent *in vitro* study, which included over 100 human breast cancer samples, reported that the NPY receptor, predominantly the Y_1 subtype, was expressed in 85% of primary carcinomas and 100% of lymph node metastases of receptor-positive primary tumors. These results are higher than those reported in a subsequent trial, in which the NPY(Y_1) receptor was observed in only 69% of the primary breast tumor samples analyzed and at high density (>2,000 dpm/mg tissue) in only 66% of those samples.

The recent development of receptor subtype selective NPY analogs, combined with novel strategies for the synthesis and radiolabeling of these analogs, has enabled progress in the construction of NPY receptor targeted radiopharmaceuticals that may be employed for breast cancer detection and diagnosis. Radiolabeling of NPY(Y_1)-selective conjugates was initially achieved by exploiting the high tyrosine content of these derivatives which allowed for the oxidative incorporation of iodine-125 (^{125}I). Although this represents a rapid and facile radiosynthetic method, it is also non-selective, allowing for the potential incorporation of ^{125}I into residues that are involved in receptor binding. In order to address this limitation, subsequent radiolabeling techniques have employed photolabile protecting groups and bifunctional chelating agents (BFCA) (Zwanziger et al., 2008).

Despite these advances in the field of NPY(Y_1) receptor imaging, proof of principle remains to be established. In fact, in a recent study which utilized NMRI nu/nu mice bearing MCF-7 tumors to analyze the biodistribution of the NPY(Y_1)-selective peptide DOTA-[Phe_7, Pro_{34}] NPY radiolabeled with indium-111 (^{111}In), tumor uptake of the conjugate was relatively low at all time points (30 minutes post-injection (p.i.) = 1.7 ± 0.5% injected dose per gram (%ID/g)). In addition, although the NPY(Y_1) receptor is found in high density in 66% of *in situ*, invasive, and metastatic breast cancers, it is also present in both the lobules and ducts of normal breast tissue, which decreases the tumor-to-background ratio and degrades the overall image resolution. Thus, the suitability of radiolabeled NPY(Y_1) receptors for the routine detection and diagnosis of breast cancer remains in question.

2.5 Gastrin releasing peptide receptor (GRPr) sScintigraphy

Gastrin releasing peptide (GRP) is a peptide hormone composed of 27 amino acids that, along with neuromedin C, are the cleavage products of a 148 amino acid preproprotein. GRP belongs to the bombesin-like (bombesin = BBN) family of peptides that regulates numerous functions in the enteric and the central nervous systems, including circadian rhythm, immune function, thermoregulation, satiety, gastrointestinal hormone release,

smooth muscle contraction, and epithelial cell proliferation (Knigge et al., 1984). These actions are mediated by binding to $G_{q/11}$ protein-coupled receptors of the bombesin family (BB_1- Neuromedin B receptor, BB_2- GRPr, BB_3- Orphan receptor, BB_4- BBN receptor) expressed in the pancreas, stomach, adrenal cortex, and brain, which activates the intracellular phospholipase C signal transduction cascade leading to inositol triphosphate (IP_3) and diacylglycerol (DAG) generation, and subsequent intracellular calcium elevation (Gugger & Reubi, 1999; Smith et al., 2005).

Of all the physiological effects of GRP, the most studied is the one related to cancer. Investigation into the role of GRP in cancer progression began with the observation in 1981 that both cancer cell lines and primary human tumors can synthesize GRP as well as its amphibian analog BBN (Moody et al., 1981). Four years later, Cuttitta et al. demonstrated that GRP and BBN stimulate the growth of small cell lung cancer, and that this ability is part of an autocrine feedback mechanism that involves the interaction of these peptides with their receptors, which are expressed on the surface of tumor cells (Cuttitta et al., 1985). The mitogenic role of GRP and BBN in other cancers has since been established, including those of the lung, pancreas, prostate, central nervous system, and breast (Reubi, 2008). While the mechanism of growth stimulation does not appear to be constant for all carcinomas, it generally involves the transactivation and up-regulation of epidermal growth factor (EGF) receptors (Van de Wiele et al., 2000).

Although GRPrs have been readily detected in various tumor cell lines, identification of these receptors in primary human tumors has proven to be more difficult. While the presence of GRPr proteins has not been conclusively established in either gastrointestinal or exocrine pancreatic carcinomas, both GRP mRNA and receptor proteins have been detected in neoplasms of the prostate and breast (Reubi, 2008). Expression of GRPrs in neoplastic epithelial mammary cells have been reported in approximately two thirds (62-71%) of all breast carcinomas, and in high density (>2,000 dpm/mg tissue) in 65% of these cases. In addition, all of the lymph node metastases from GRPr-positive primary breast carcinomas were positive for this receptor, whereas the surrounding lymphoreticular tissue was GRPr-negative. Although GRPrs are present in both the ducts and lobules of nonneoplastic breast tissue, their heterogeneous distribution, coupled with the strong GRPr expression by primary breast carcinomas as well as metastatic sites, indicates that breast cancer may be effectively imaged using GRP and BBN analogs (Gugger & Reubi, 1999; Reubi, 2008).

For over a decade, the feasibility of using radiolabeled BBN analogs to detect and diagnose GRPr-positive breast cancer has been investigated. The translation of these efforts into human subjects first occurred in 2000, with the publication of the results from the first human trial (Van de Wiele et al., 2000). In order to evaluate the diagnostic utility of ^{99m}Tc-RP527, Van de Wiele et al. administered this agent to six patients with metastatic breast cancer prior to image acquisition (planar, SPECT). While low physiological uptake of ^{99m}Tc-RP527 was observed in normal breast tissue, it did not affect the visualization of either the primary tumor or metastatic sites, which were successfully imaged in 4 out of 6 patients with tumor-to-background ratios of 1.7 to 3.4 and 2.6 to 7.2 at 1 and 6 hours p.i., respectively. Similar results were obtained by Scopinaro et al. in a 2002 trial which compared the diagnostic capacity of a ^{99m}Tc-labeled BBN analog with that of ^{99m}Tc-sestamibi in five patients with infiltrating ductal carcinoma (Scopinaro et al., 2002). Although the identification of metastatic sites was achieved with both agents, detection of the primary tumor was higher for ^{99m}Tc-BBN (100%) than for ^{99m}Tc-sestamibi (80%). This may be related to the higher affinity of BBN analogs for malignant breast tissue which often over-express

the GRPr, allowing for improved tumor-to-background ratios when compared with ^{99m}Tc-sestamibi (1.4-2.3 vs. 1.0-1.8 at 5 minutes) (Scopinaro et al., 2002). While the results of these trials indicate that the detection/diagnosis of both primary breast cancer and metastatic sites can be achieved using radiolabeled BBN derivatives, the disadvantages demonstrated by these agents (moderate tumor-to-background ratios, hepatobiliary excretion) need to be addressed in order to recognize their full potential.

2.6 GRPr-expressing T-47D human bBreast cancer cells

The ability of radiolabeled BBN analogs to detect and diagnose both primary breast carcinomas and metastatic sites which express the GRPr, coupled with the expression of this receptor in 62-71% of breast cancer cases, has fueled continued interest in the development of BBN-based tumor targeting agents. In order to produce high quality SPECT images, radiotracer accumulation and residualization in GRPr-expressing cells must be maximized to optimize the contrast and hence the resolution of the resulting image. While there are other cell lines that express the GRPr in relative high numbers, our group and many others have used the T-47D human breast cancer cell line in a variety of studies to evaluate the therapeutic and diagnostic efficacy of potential radiopharmaceuticals. This differentiated cell line, with breast epithelial morphology, was derived from a metastatic pleural effusion originating from an infiltrating ductal carcinoma in a 54 year-old Caucasian patient (Lacroix & Leclercq, 2004; Engel & Young, 1978). The cell line is described as "luminal epithelial-like" with markers indicating its pre-metastatic state according to the EMT (epithelial-mesenchymal transition) hypothesis for metastatic transformation. It has been shown that the GRPR is over-expressed on the surface of T-47D breast carcinoma cells while being absent from normal breast tissues (Giacchetti et al., 1990). This receptor has served as a target for a number of diagnostic and therapeutic strategies (Prasanphanich et al., 2007; Garrison et al., 2007; Parry et al., 2007; Biddlecombe et al., 2007; Guojun et al., 2008; Zhou et al., 2003; Ma et al., 2007). T-47D xenografts in mice have been used in preclinical investigations of a variety of diagnostic modalities (Giblin et al., 2006; Aliaga et al., 2004).

T-47D Cell Line	
Cell Line Origin	Female patient. Age = 54. Pleural effusion from an invasive ductal carcinoma.
Acquisition Data	Dr. Keydar, 1974
In Vitro Invasion	Positive (low)
Estrogen Receptor	Positive
Progesterone Receptor	Positive
GRPr	Positive (36,000 sites/cell)
^{125}I-Tyr^4-BBN(7-14)NH_2: Binding Capacity and Affinity	$9.7x10^{-13}$M/mg K_D = 1 nM

Table 2. T-47D Cell line characteristics (Giacchetti et al., 1990)

3. Site-directed radiopharmaceutical composition

The use of peptide-based bioconjugates in molecular investigations is common. Typically, a peptide is covalently modified with a bifunctional chelating agent (BFCA) capable of

complexing and stabilizing a radionuclide. Pharmacokinetic modifiers can be introduced between the peptide and the BFCA to fine-tune the biodistribution of the bioconjugate. The potential of using peptide-based site-directed radiopharmaceuticals for *in vivo* single-photon emission computed topography (SPECT) and PET imaging has recently become apparent (Sprague et al., 2007; Weiner & Thakur, 2005).

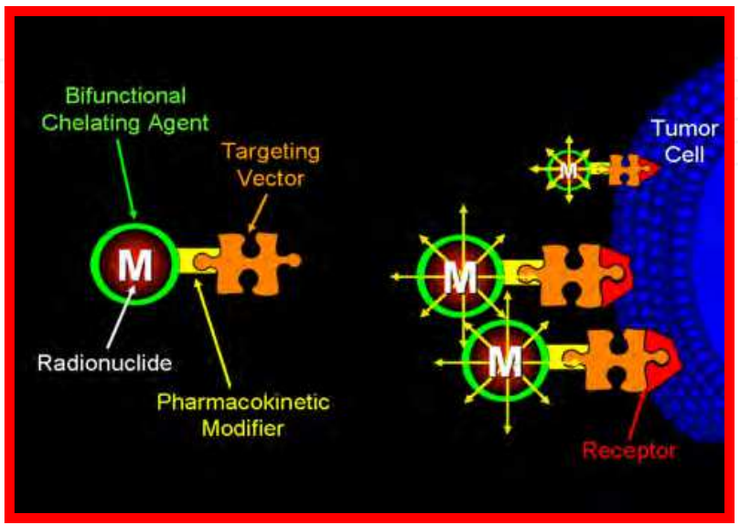

Fig. 1. Schematic representation of a radiolabeled targeting vector for treatment of human disease.

3.1 Bombesin targeting vectors

Radiopharmaceuticals designed to target the GRPr employ modified analogs of bombesin, a tetradecapeptide initially isolated from the skin of the fire-bellied toad *Bombina bombina* in 1971 (Reubi, 2008; Smith et al., 2003; Zhang et al., 2004). The amidated C-terminus sequence of seven amino acids (**Trp-Ala-Val-Gly-His-Leu-Met-NH_2**), which is homologous to that of GRP (Table 3), is utilized for conjugate synthesis as a result of the fact that this sequence is sufficient for specific high affinity binding to the GRPr.

GRP	Val-Pro-Leu-Pro-Ala-Gly-Gly-Gly-Thr-Val-Leu-Thr-Lys-Met-Tyr-Pro-Arg-Gly-Asn-His-**Trp-Ala-Val-Gly-His-Leu-Met-NH_2**
BBN*	Pyr-Gln-Arg-Leu-Gly-Asn-Gln-**Trp-Val-Gly-His-Leu-Met-NH_2** Pyr-Gln-Arg-Leu-Gly-Asn-Gln-**Trp-Ala-Val-Gly-His-Phe-Met-NH_2**

*Two distinct forms of BBN have been identified for the BB_4 receptor subtype.

Table 3. Amino Acid Sequence Comparison, GRP versus BBN (Smith et al., 2003)

The utilization of radiolabeled receptor agonists for cancer detection, diagnosis, and treatment has traditionally been accepted due to the fact that agonists often undergo rapid internalization upon receptor binding and are subsequently residualized within the tumor cell for an extended period of time. The internalization mechanism for BBN-based agonists involves the endocytosis of the agonist/GRPr complex into clathrin-coated vesicles and endosomes. This is followed by migration to the perinuclear space where lysosomal entrapment of the agonist occurs, prolonging the residence time of agonist-bound

radioactivity in the target tissue. This allows for the accumulation of radioactivity in GRPr-positive tissues, thereby facilitating breast cancer diagnosis and treatment (Van de Wiele et al., 2000). While a number of BBN-based agonists have been developed, in order to maintain a high binding affinity for the GRPr subtype, these analogs all contain the seven amino acid GRPr binding motif with limited substitution (Coy et al., 1988; Pomper & Gelovani, 2008). The production of radiopharmaceutial agents from these BBN(7-14)NH_2 based compounds may be readily achieved using a variety of radiometal chelates. The resulting radiotracers have been demonstrated to retain high specific binding to the GRPr in a variety of human cancer cell lines, including those of the prostate, pancreas, and breast (Inhibitory Concentration at 50% (IC_{50}) = 1-10 nM).

3.2 Pharmacokinetic modification—"Linking groups"

An important aspect in the design of new radiopharmaceuticals is the adjustment of the pharmacokinetic properties of an agent, which influence its biodistribution and clearance. These factors have a significant impact on the tumor-to-background ratio, and hence the diagnostic and therapeutic utility that will be exhibited by a radiotracer. While the GRPr binding motif is not generally modified during conjugate production, amendments to this basic sequence are commonly employed for a number of reasons including augmentation of conjugate resistance to degradation by plasma peptidases, alteration of the pharmacokinetic properties of the derivative, and facilitation of the radiolabeling procedure (Blok et al., 1999; Signore et al., 2001).

Incorporation of an inert spacer group into a BBN-based radiopharmaceutical is an effective method of modifying both the physiochemical properties and the metabolic fate of the bioconjugate, improving both the residualization of radioactivity by GRPr-positive malignant cells and clearance of the radiotracer from the blood and non-target tissues (Pomper & Gelovani, 2008). Both length and charge of the spacer group influence the pharmacokinetic properties, GRPr binding affinity, and tumor uptake of the BBN analog. Addition of a peptide sequence such as polyglycine or polyserine can be used to augment the hydrophilicity of a conjugate, thereby enhancing renal clearance, while the incorporation of a simple hydrocarbon chain may be employed to increase its lipophilicity in order to prolong its residence time in the bloodstream. An alternative approach to reduce the circulatory clearance rate of an analog is the insertion of a polyethyleneglycol (Peg) linker, which slows the extraction of the conjugate by hepatocytes (Krause, 2002). In the case of BBN(8-14)NH_2 based analogs, the incorporation of a tethering moiety between the receptor binding sequence and the radiometal complex influences not only the pharmacokinetic properties and renal retention of the resulting conjugate, but also the binding affinity and the degree of receptor-mediated analog uptake that is observed in GRPr rich tissues. In order to maintain a GRPr binding affinity that is similar to native BBN, the receptor binding sequence and the radiometal chelate must be separated by a distance of five or more atoms and the spacer sequence employed to serve this purpose must not introduce an extra negative charge at the N-terminus (Hoffman et al., 2001; Zhang et al., 2004).

Additionally, a spacer group creates distance between the appended radiometal chelate and the receptor binding sequence, which promotes the biological integrity of the radiotracer (Pomper & Gelovani, 2008). As both the receptor binding sequence and the C-terminus are essential to the *in vivo* interaction between BBN-based conjugates and the GRPr, attachment of the tethering moiety occurs at the N-terminal tryptophan in position 8 (Trp^8). Spacer

group selection is critical because the effect of side chain conjugation to the Trp^8 residue is unpredictable. The attachment of some amino acid chains or other groups has been demonstrated to dramatically decrease the binding affinity of the BBN analog (Coy, et al., 1988). To avoid this issue, glutamine is frequently appended to the Trp^8 residue prior to the addition of the linker as its inclusion is not only compatible with maintaining high GRPr binding affinity, but also with reducing the renal retention of the resulting BBN(7-14)NH_2 conjugate (Hoffman et al., 2001).

3.3 Radiolabeling techniques and bifunctional chelating agents (BFCAs)

Radiolabeling may result in substantial alterations to both the lipophilicity and the charge of the radiopharmaceutical and has important consequences for both the biodistribution and the kinetic properties of the resulting agent (Blok et al., 1999; Signore et al., 2001). For instance, the introduction of a negative charge at the N-terminus of a BBN analog leads to a loss of binding affinity, while a positive charge augments it, resulting in the potential for increased accumulation in GRPr rich tissues. Radioisotope complexation to biologically active peptide based targeting vectors may be accomplished *via* either direct or indirect radiolabeling approaches (Stigbrand et al., 2008). While there are distinct advantages and disadvantages associated with each of these methods, the production of high specific activity products is essential to the generation of high resolution scintigraphic images.

Direct radiolabeling is a relatively rapid, facile synthetic method that utilizes functional groups, such as sulfhydryls or thioethers, which are present within the peptide to complex the radioisotope. However, this technique often suffers from a lack of specificity as the location of radioisotope incorporation into the resulting radiopharmaceutical may involve functional groups within or near the receptor binding sequence. This can decrease the affinity of the conjugate for its receptor, resulting in diminished accumulation in target tissues, which reduces the resolution, and hence the diagnostic utility of the scintigraphic image that is produced.

Indirect radiolabeling overcomes many of these difficulties by employing a bifunctional chelating agent (BFCA) to complex the radioisotope, providing distance between the metal chelate and the receptor binding sequence in order to preserve the biological activity of the radiopharmaceutical. BFCAs are designed not only to form stable, high yield complexes with metallic radionuclides, but also to covalently link these radioisotopes to the targeting vector. The BFCA may be conjugated to the targeting vector either prior to or subsequent to the radiolabeling procedure. In the pre-conjugation technique, synthesis of the BFCA-radiometal complex occurs in advance of conjugation to the targeting vector. This method is employed when the BFCA-radionuclide complex can only be generated under harsh reaction conditions, such as extreme temperature or pH, which may destroy the receptor binding region of the molecule (Stigbrand et al., 2008). The preferred method of indirect radiolabeling is the post-conjugation approach as it represents an effective, one-step method of radiopharmaceutical synthesis in which the BFCA is directly conjugated to the targeting vector prior to radioisotope complexation. Ideally, only specific donor atoms of the BFCA will coordinate the radiometal to produce a high yield conjugate with both high receptor affinity and *in vivo* stability. In order to achieve a high degree of *in vivo* stability, the BFCA must impart both thermodynamic and kinetic inertness to the resulting radiometal complex. This serves to decrease not only the *in vivo* metabolism of the radiopharmaceutical but also the subsequent retention of these metabolites by non-target tissues such as the stomach, liver, and kidneys, thereby increasing the tumor-to-background ratio.

4. microSPECT imaging using technetium-99m-BBN agents

Although a multitude of radioisotopes have been utilized in the development of diagnostic radiopharmaceuticals, ^{99m}Tc remains the most widely employed radionuclide in diagnostic nuclear medicine, accounting for approximately 85% of all nuclear medicine procedures performed (Smith et al., 2003). Technetium-99m is well suited for use as a radionuclide due to its ready availability *via* on site ^{99}Mo/^{99m}Tc generator systems, ideal nuclear characteristics (half-life ($t_{1/2}$) = 6.04 hours, gamma energy = 140.5 keV (89%), high specific activity), favorable dosimetry, and well-established labeling chemistries using a variety of BFCAs (Fischman et al., 1993; Smith et al., 2003 and 2005; Varvarigou et al., 2004). In addition, the chemistry of ^{99m}Tc is parallel to that of the therapeutic radioisotopes $^{186/188}$Re, allowing for the development of diagnostic/therapeutic radiopharmaceutical pairs. As such, the diagnostic agent may be employed in prescreening patients prior to therapy, which would provide valuable individual information regarding drug pharmacokinetics, receptor density, and dosimetry, potentially reducing or even eliminating unsuccessful radiotherapeutic regimens.

While ^{99m}Tc can exist in a variety of oxidation states ranging from +7 to -1, it is most stable in the +7 state (i.e. TcO_4^-, pertechnetate). Lower oxidation states may be stabilized by complexation with numerous ligands, resulting in radiometal chelates that have coordination numbers between 4 and 9. While oxidation states below +4 are easily oxidized to the +4 state, ^{99m}Tc in the +5 and +6 states frequently undergoes disproportionation into the +4 and +7 states, respectively. However, the type of complex formed and its stability are highly dependent on labeling conditions, which include pH, BFCA, reducing agent, and concentration. Initially, ^{99m}Tc chemistry focused on the +5 oxidation state as it may be complexed using a broad range of thiol-, isonitrile-, or phosphine-containing chelates to produce compounds that are highly stable in aqueous media (Blok et al., 1999). However, it is often difficult to produce well-defined conjugates with high specific activity *via* direct or indirect radiolabeling techniques, due to the fact that the reduction of the disulfide bonds in the targeting vector or the ligand framework may occur as a consequence of the presence of excess reducing agent (Sn^{2+}) in the labeling cocktail (Schibli & Schubiger, 2002). In addition, the resulting derivatives frequently suffer from significant *in vivo* hydrophobicity, prolonging their residence time in both the circulatory system and non-target tissues, which decreases the target-to-background ratio, and hence the resolution, of the resulting scintigraphic image, while simultaneously increasing the radiation exposure to the patient (Smith et al., 2003).

Both of these issues have been addressed utilizing the organometallic tricarbonyl core, *fac*-^{99m}Tc$(CO)_3$, formulated in the late 1990s (Alberto et al., 1998). Although initially the *fac*-$[^{99m}Tc\text{-}(H_2O)_3(CO)_3]^+$ precursor was obtained by direct carbonylation of the permetallate salt ($Na[TcO_4]$) using sodium borohydride under atmospheric carbon monoxide pressure, a method was subsequently devised for the fully aqueous, normal pressure preparation by employing potassium boranocarbonate ($K_2[H_3BCO_2]$) as both the reducing agent and the source of carbon monoxide (Alberto et al., 2001; Schibli & Schubiger, 2002). This method eliminates undesired disulfide bond reduction in the conjugates because excess reducing agent is destroyed prior to the radiolabeling procedure. The synthetic ease, high yield, excellent radiochemical purity, reproducibility, and improved safety associated with this new method of radiolabeling using the tricarbonyl core spurred the development of a commercial kit (Isolink®) for $[^{99m}Tc\text{-}(H_2O)_3(CO)_3]^+$ preparation (Biersack & Freeman, 2007).

The remarkable kinetic and thermodynamic stability demonstrated by the $[^{99m}Tc\text{-}(H_2O)_3(CO)_3]^+$ aqua ion in aerobic, aqueous solutions over a wide range of pH values is derived from two factors: 1) the shape of the ^{99m}Tc-labeled precursor, and 2) the oxidation state of ^{99m}Tc. The $^{99m}Tc(CO)_3$ metal core is compact, with an almost spherical shape, which if "closed" with an appropriate ligand system will form an octahedral coordination sphere that effectively protects the metal center against further ligand attack or reoxidation. Conversely, $^{99m}Tc(V)$-complexes possess an "open" quadratic pyramidal structure, which is prone to ligand attack and/or protonation often resulting in decomposition of the original complex (Schibli & Schubiger, 2002). In addition, $^{99m}Tc(I)$ has a low spin d^6 electron configuration that is responsible for the octahedral shape of these complexes, endowing them with large crystal field stabilization energies in the presence of strong field ligands such as CO, further contributing to the kinetic and the thermodynamic stability of these compounds. Unlike the CO ligands in the aqua ion, the water ligands are not π-electron acceptors and as a result their binding to the metal center is not stabilized by synergic bonding. This accounts for the substitution lability of these ligands which can undergo facile exchange reactions with a number of donor groups including amines, thioethers, phosphines, and thiols (Jones & Thornback, 2007). The ease of these reactions contributes to the excellent labeling efficiencies exhibited by the $[^{99m}Tc\text{-}(H_2O)_3(CO)_3]^+$ precursor, which results in the production of metallated conjugates with remarkable *in vitro* and *in vivo* stability against serum-based proteins and superior uptake and retention when compared with $^{99m}Tc(V)$- agents.

In recent studies, we have evaluated conjugates of the type DPR-Y-BBN(7-14)NH_2 where DPR = 2,3-diaminopropionic acid (DPR), and Y= GSG or SSS (Retzloff et al., 2010) that when radiolabeled with *fac*-$[^{99m}Tc\text{-}(H_2O)_3(CO)_3]^+$ produced metallated conjugates $^{99m}Tc\text{-}(CO)_3$-DPR-Y-BBN(7-14)NH_2 in very high yield (~90%) (Figure 2) These products demonstrated *in vitro* stability in excess of 24 hours as monitored by reverse phase-high performance liquid chromatography (RP-HPLC), with no observable degradation or transchelation to inherent functional donor atoms present in either histidine solution (1 mM) or human serum albumin.

In competitive radioligand binding assays against ^{125}I-[Tyr^4]-BBN(7-14)NH_2, the standard for the evaluation of GRPr specific binding, these derivatives demonstrated very high affinities for the GRPr, with IC_{50} values of 8.1 ± 1.3 nM for Y = GSG, and 5.9 ± 0.8 nM for Y = SSS in the T-47D cell line (Retzloff et al., 2010). The internalization and externalization (trapping) of the $^{99m}Tc\text{-}(CO)_3$-DPR-Y-BBN(7-14)NH_2 derivatives, when assessed in T-47D cell lines showed that the apex of internalization occurred between 45 and 120 minutes, when uptake levels reached 80-88% of all cell-associated radioactivity in the T-47D cell line. This level of internalization remained relatively constant for subsequent time points, with no significant efflux of radiotracer observed over a 90-minute period.

Results obtained from biodistribution studies in SCID mice bearing human T-47D xenografted tumors suggested that analog size and lipophilicity strongly influence *in vivo* pharmacokinetic behavior. While the $^{99m}Tc\text{-}(CO)_3$-DPR-Y-BBN(7-14)NH_2 derivatives were eliminated primarily *via* the renal-urinary system, both the rate and the extent of clearance was affected by the DPR BFCA and the amino acid spacer sequence of the derivative. The prompt elimination of the DPR analogs from the body, where Y = GSG or SSS, can be attributed to the small size and hydrophilic nature of both the DPR BFCA and the amino acid linkers which served to mitigate the lipophilic character of the $^{99m}Tc(CO)_3$ metal core. As a result of this clearance pattern, these $^{99m}Tc\text{-}(H_2O)(CO)_3$-DPR-Y-BBN(7-14)$NH_2$ analogs

demonstrated consistently lower levels of background radioactivity in non-target tissues, such as the liver and the gastrointestinal tract. In addition to aiding in their prompt elimination *via* the renal-urinary pathway, the small size and hydrophilic nature of the DPR derivatives containing amino acid linkers allowed for the rapid penetration of these conjugates into GRPr-positive target tissues, as evidenced by their comparatively high levels of uptake by both GRPr-expressing pancreatic and tumor tissues. Tumor uptake and retention in T-47D xenografted breast cancer tumors were 2.3-2.4 ± 0.4-0.8% ID/g (Y = GSG) and from 2.4-3.7 ± 0.7-1.8% ID/g (Y = SSS) at 1 hour p.i., respectively.

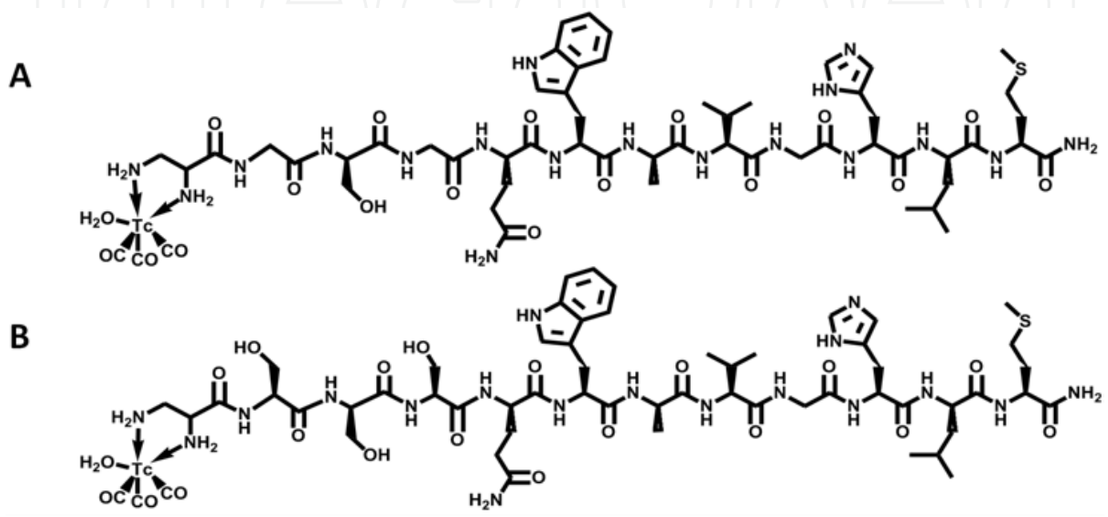

Fig. 2. ^{99m}Tc-$(CO)_3$-(H_2O)-DPR-GSG-BBN(7-14)NH_2 (A) and ^{99m}Tc-$(CO)_3$-(H_2O)-DPR-SSS-BBN(7-14)NH_2 (B) conjugates.

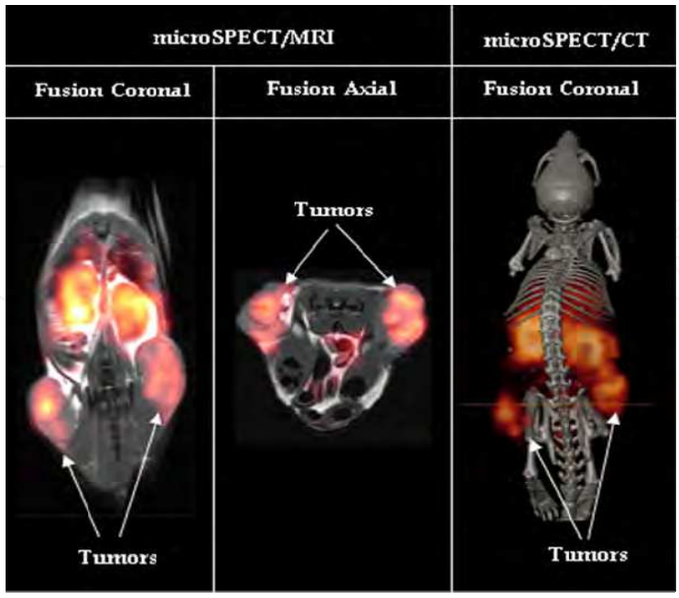

Fig. 3. microSPECT/MRI/CT imaging of ^{99m}Tc-$(H_2O)_3(CO)_3$-DPR-SSS-BBN(7-14)NH_2 after 24 h p.i.

Due to each rapid elimination from non-target tissues *via* the renal-urinary excretion pathway and moderate accumulation and retention in tumor tissue, ^{99m}Tc-$(H_2O)(CO)_3$-DPR-Y-BBN(7-14)NH_2 conjugates were evaluated for microSPECT imaging in T-47D tumor-bearing SCID mice at 24 hours p.i.(Figure 3). These conjugates produced favorable tumor-to-background ratios, which allowed for clear visualization of tumor tissue, despite some level of background radioactivity. Although the location and intensity of this background radioactivity fluctuated slightly among these conjugates, the kidneys and the gastrointestinal tract were consistently the predominant sources of radioactivity at the time of imaging. Despite these subtle differences in biodistribution, clear identification of tumor tissue was readily achieved with both derivates, supporting the hypothesis that radiolabeled ^{99m}Tc(I)-BBN conjugates may be employed to diagnose GRPr-expressing breast cancers.

5. microPET imaging with copper-64-BBN conjugates

While a variety of diagnostic imaging techniques exist for identifying breast cancer, low-dose mammography is still considered to be the most accurate and dependable procedure (Prasad & Houserkova, 2007). Still, digital mammography is most accurate in women under 50, with low-density breast, who have either not entered or recently passed through menopause (Pisano et al., 2005). PET imaging using FDG (^{18}F-fluorodeoxyglucose) has been an effective technique for diagnosis of primary breast cancer and benefited from PET imaging devices designed specifically for breast imaging. While FDG-PET was able to identify tumors in the breast, a high false-positive rate, 87%, limits its wide-spread use. (Kaida et al., 2008). Thus there is a need to develop diagnostic modalities with increased specificity for malignant breast tissues and capable of overcoming these limitations. Targeting a unique physiological manifestation of breast malignancy, such as over-expression of an extracellular receptor with a diagnostic radionuclide, might be a procedure capable of imaging tumors of the breast with higher resolution and lower false-positive rates.

Copper-64 is one of few radionuclides possessing physical properties that allow for medical imaging and therapy (Nijsen et al., 2007). The utility of ^{64}Cu ($t_{1/2}$ = 12.7 h, cyclotron generated as $^{64}CuCl_2$) results from its diverse decay profile. Electron capture, with corresponding gamma emission at 1346 keV, accounts for 41% of the decay profile for ^{64}Cu. This is accompanied by emission of a β^- particle (40%, 190 keV) and a positron (β^+, 19%, 278 keV). The degree of β^+ decay is sufficient for PET imaging *in vivo* and has been extensively investigated. Moreover, ^{67}Cu-containing radiopharmaceuticals possess therapeutic potential and provide *in vivo* pharmacokinetic profiles nearly identical to ^{64}Cu-containing drugs (Blower et al., 1996). ^{67}Cu has ideal physical characteristics that are well-suited for radionuclide therapy (β^-, 100%, 121 keV, $t_{1/2}$ = 62 h) (Voss, et al., 2007). As such, ^{64}Cu can be used as a dose-determinant indicator in ^{67}Cu-based therapeutic regimens.

While the physical properties of copper are well-suited for use in radiopharmaceuticals, the metabolism and physiological properties of copper in the human body present a challenge to the development and wide-spread use of copper-containing radiopharmaceuticals. Ideally, site-directed radiopharmaceuticals accumulate at the target site quickly with little accumulation in non-target tissues and rapidly clear non-target tissues after administration. Hence, hepatobiliary clearance of radiopharmaceuticals is much less desirable to renal/urinary clearance. Since the liver is the anatomical location of copper metabolism, the stability of the copper chelate in a ^{64}Cu-containing radiopharmaceutical under physiological

conditions is very important (Wadas et al., 2007). Increasing the stability of copper complexes *in vivo* has been a major focus in the field of nuclear medicine for some time (Di Bartolo et al., 2001 and 2006; Gasser et al., 2008; Kukis et al., 1993; Voss et al., 2007; Pippin et al., 1991; Geraldes et al., 2000; Wieghardt et al., 1982; van der Merwe et al., 1985; Prasanphanich et al., 2007; Soluri et al., 2003; Maina et al., 2005; Monstein et al., 2006; Sun & Chen, 2007) as the development of stable copper complexes will allow for a variety of copper-based diagnostic and therapeutic strategies.

Recent work in the field of copper radiochemistry has produced very promising results. A majority of the work has focused on synthesis of new ligand frameworks to chelate copper in a multi-dentate fashion to prevent loss of the Cu^{2+} ion under *in vivo* conditions. Cross-bridged TETA (1,4,8,11-tetraazacyclotetradecane-1,4,8,11-tetracetic acid) derivatives, such as 4,11-bis(carboxymethyl)-1,4,8,11-tetraazabicyclo[6.6.2]hexadecane (CB-TE2A) and 1-N-(4-aminobenzyl)-3,6,10,13,16,19-hexa-aza-bicyclo-[6.6.6]eichosane-1,8-diamine (SarAr), have shown increased copper-complex stability *in vivo* versus the TETA and DOTA (1,4,7,10-tetraazacyclododecane-1,4,7,10-tetraacetic acid) chelators (Garrison et al., 2007; Di Bartolo et al., 2001 and 2006). Additionally, derivatives of the triazacyclononane macrocycle have produced improved stability of copper complexes (Prasanphanich et al., 2007). Pippin et al., have shown that complexes of Cu(II) with NOTA (1,4,7-triazacyclononane-1,4,7-triacetic acid) are more inert towards isotopic exchange with ^{67}Cu than DOTA or TETA (Pippin et al., 1991). Recent work by Gasser, et al., demonstrated a 2-[4,7-bis(2-pyridylmethyl)-1,4,7-triazacyclononan-1-yl] acetic acid (PMCN) bifunctional chelator containing the ^{64}Cu radionuclide (Gasser et al., 2008). Recently, we have reported on the superior microPET imaging quality of NOTA bifunctional chelator over that of the DOTA using ^{64}Cu in a GRPR-positive human prostate cancer mouse model (Prasanphanich et al., 2007). Previous investigations have reported a highly stable complex consisting of NOTA and divalent copper (Kukis et al., 1993; Geraldes et al., 2000; Wieghardt et al., 1982). Also reported are biomolecules conjugated with NOTA and chelating ^{64}Cu. Interestingly, one investigation reported a crystal structure of [CuCl(TACNTA)-], or [CuCl(NOTA)-], with a pentadentate NOTA in which one carboxylate arm of the triazacyclononane macrocycle is not involved in the coordination of copper(II) (van der Merwe et al., 1985). This implies that occupation of this non-chelating carboxylate of NOTA, as in our bifunctional NO2A, may not alter the native structure of the Cu-NOTA complex.

We have recently evaluated ^{64}Cu-NO2A-8-Aoc-BBN(7-14)NH_2 radiopharmaceutical (Figure 4) to be used as a PET targeting agent for primary or metastatic breast cancer disease (Prasanphanich et al., 2009). In this study, we were able to prepare high specific activity ^{64}Cu-NO2A-8-Aoc-BBN(7-14)NH_2 conjugate in very high radiochemical yield and to evaluate the 1) targeting capacity of ^{64}Cu-NO2A-8-Aoc-BBN(7-14)NH_2 for GRPr-positive tissues *in vivo*; 2) particular routes of clearance; and 3) extent of retention of radiopharmaceutical in radiosensitive tissues.

A number of *in vitro* assays were used to evaluate the uptake and affinity of ^{64}Cu-NO2A-8-Aoc-BBN(7-14)NH_2 for the GRPr in T-47D human breast cancer cells. Competitive binding displacement assays using ^{125}I-[Tyr^4]-BBN(7-14)NH_2, as the radioligand were used to quantify the relative binding affinity of Cu-NO2A-8-Aoc-BBN(7-14)NH_2 for GRPrs located on the surface of T-47D cells. The concentration of Cu-NO2A-8-Aoc-BBN(7-14)NH_2 needed to inhibit ^{125}I-[Tyr^4]-BBN(7-14)NH_2 binding by 50% was determined to be 7.56 ± 2.23 nM. The rate at which cell-associated radioactivity was internalized within the T-47D cells was also measured. After incubating T-47D cells in media containing ^{64}Cu-NO2A-8-Aoc-BBN(7-

14)NH_2 for 45 min, nearly 90% of all cell-associated radioactivity had internalized. This remained nearly constant for subsequent time points. The externalizaton of ^{64}Cu-NO2A-8-Aoc-BBN(7-14)NH_2 from T-47D cells was measured by removing cells from conjugate-containing media after 45 min and washing them to remove all surface-bound radioactivity. No significant efflux of radiotracer was observed over the 90 min period.

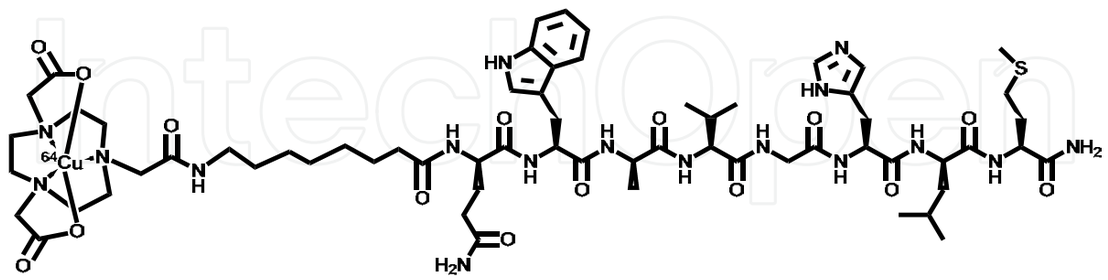

Fig. 4. ^{64}Cu-NO2A-8-Aoc-BBN(7-14)NH_2 conjugate.

Results obtained from biodistribution studies in SCID mice bearing human T-47D xenografted tumors suggested uptake in GRPr expressing tissues was receptor mediated. The average uptake and retention of conjugate in T-47D xenografted tumors at 1, 4, and 24 h p.i. were 2.27 ± 0.08, 1.35 ± 0.14, and 0.28 ± 0.07% ID/g. The primary mode of excretion for this conjugate was the renal-urinary excretion pathway. A receptor blocking assay in which BBN(1-14)NH_2 was administered 15 min prior to targeting vector in T-47D tumor-bearing mice showed a significant decrease in the accumulation of ^{64}Cu-NO2A-8-Aoc-BBN(7-14)NH_2 in tumor tissue. For example, uptake/accumulation of ^{64}Cu-NO2A-8-Aoc-BBN(7-14)NH_2 conjugate was reduced to 0.58±0.10% ID/g (1 h p.i.) with the addition of the blocking agent to the study. Furthermore, in the blocking assay, the degree of urinary excretion increased to 82 ± 18% ID and suggests that the radioactivity detected in the intestines were at least partially the result of a receptor-mediated process located along the lower gastrointestinal tract and not solely a function of hepatobiliary excretion. Additionally, accumulation of radiotracer in pancreatic tissue and tumors was significantly decreased in this blocking experiment, suggesting that the ^{64}Cu-NO2A-8-Aoc-BBN(7-14)NH_2 conjugate is intact and that GRPr-mediated binding is facilitating uptake in the tissues.

As a result of optimal uptake and retention of ^{64}Cu-NO2A-8-Aoc-BBN(7-14)NH_2 in T-47D xenografted tumor, microPET/MicroCT/microMRI multimodal imaging experiments were conducted in tumor-bearing mice (Figure 5). A SCID mouse bearing T-47D xenografted tumors on the left and right hind flanks underwent microMR and microPET/CT imaging 24 h following injection with 5.1 mCi of ^{64}Cu-NO2A-8-Aoc-BBN(7-14)NH_2. Anatomical structures observed *via* microPET imaging were consistent with pharmacokinetic data obtained from *in vivo* experiments. For example, tumors, pancreas, liver and kidneys, to a lesser extent, were clearly identifiable *via* microPET imaging analysis. Analysis of MRI data indicated small necrotic regions in the xenografted tumors as evident by increased water diffusivity. Observable in the microPET data were regions of reduced intensity that correlated well to these necrotic regions of the tumors. Additionally, the liver is observed to lack a uniform intensity. The drop in intensity correlates to the separation between the median and left lobes of the liver. The identification of such fine structures in the microPET data is a goal of diagnostic nuclear medicine. High-resolution imaging may aid in identifying structural boundaries as well as possible malignant sites.

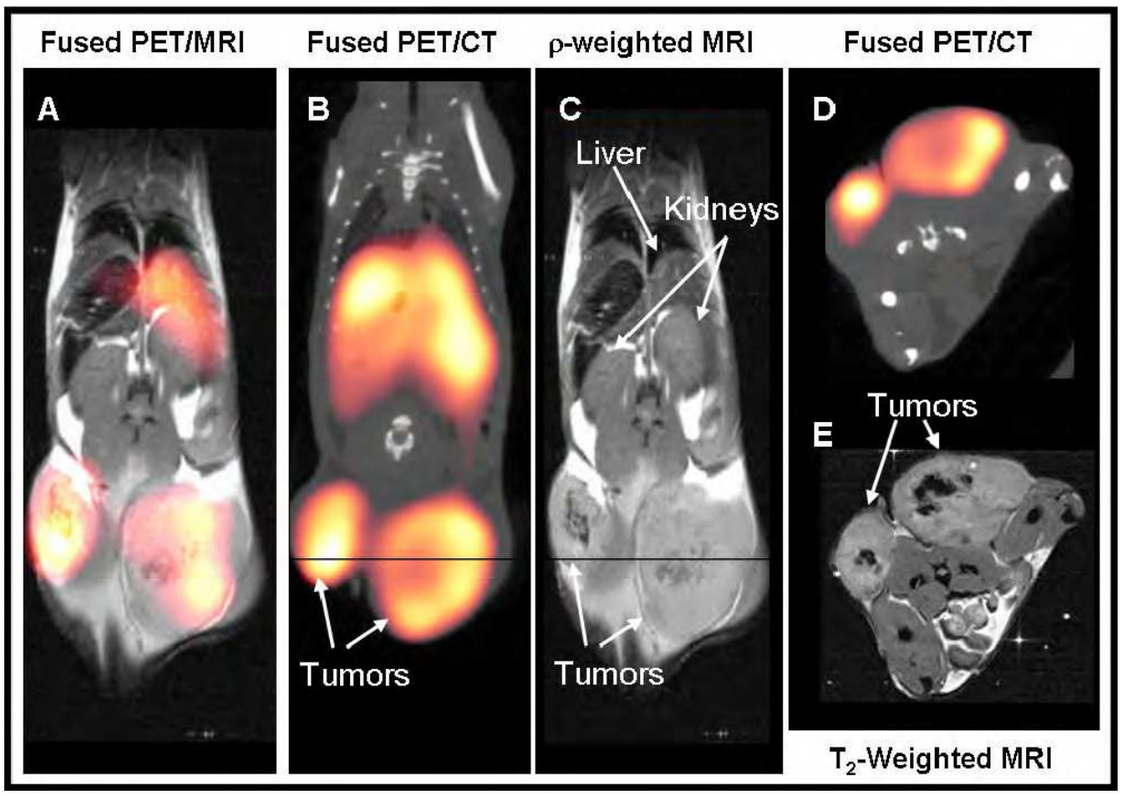

Fig. 5. *In vivo* microPET/CT and microMRI images of a T-47D tumor-bering mouse 24 h after 5.1 mCi tail vein injection of ^{64}Cu-NO2A-8-Aoc-BBN(7-14)NH_2 conjugate. (A) MicroPET/MRI fusion coronal image. (B) MicroPET/CT fused coronal image showing specific uptake of ^{64}Cu-NO2A-8-Aoc-BBN(7-14)NH_2 conjugate. (C) Proton density-weghted microMRI coronal image. (D) An axial cross section of microPET/CT images showing functional image of tumor uptake. (E) The corresponding high-resolution T2-weighted microMRI axial image correlating anatomical features of the xenografted tumors to (D).

6. Fluorescence molecular imaging using alexa fluor 680-BBN conjugates

Alternative optical imaging technologies such as fluorescence molecular tomography are emerging as new and exciting molecular imaging tools for diagnosis of human disease (Montet et al., 2006; Young & Rozengurt, 2005; Pu et al., 2005). Studies show that the high-throughput signal afforded by fluorescence imaging might offer an alternative to traditional tomographic imaging by alleviating many of the imaging artifacts seen in imaging systems of this general type (Weissleder & Ntziachristos, 2003; Zacharakis et al., 2005; Kwon et al., 2005). Therefore, design and development of new site-directed, fluorescent, targeting vectors for dynamic optical imaging of human cancers holds some significance.

Monet and co-workers have described a new peptide-nanoparticle conjugate based upon bombesin that may be potentially useful for imaging pancreatic ductal adenocarcinoma. They reported the ability of this new conjugate to specifically target GRPrs expressed on normal pancreatic tissue with minimal accumulation in normal and surrounding tissues. Furthermore, the utility of this new conjugate to be used as a dual modality MRI contrast agent was shown *in vivo* in T2 weighted MR images of rodents bearing MIA-PaCa2

pancreatic tumors (Montet et al., 2006). This study well demonstrates the potential of dual-modality imaging for diagnosis of human cancers. Young and co-workers have recently described the use of quantum dots conjugated to bombesin to successfully image living mouse Swiss 3T3 and Rat-1 cells *in vitro* (Young & Rozengurt, 2005) and Pu et al., have described a new Cypate-bombesin Peptide Analogue Conjugate (Cybesin) that has potential use as a prostate tumor receptor-mediated contrast agent (Pu et al., 2005). All of these studies provide either *in vivo* or *in vitro* evidence for production of fluorescence-based targeting vectors of bombesin for early detection of human cancers. In addition, fluorescence molecular tomography shows advantages as a relatively low cost, noninvasive procedure that utilizes highly sensitive, non-ionizing probes for tissue targeting.

To complement our work using technetium-99m and copper-64 tagged bombesin tracers to image T-47D breast cancer cells, we developed a new non-radioactive, fluorescent probe based upon BBN having high tumor uptake and optimal pharmacokinetics for specific targeting and optical imaging of the same cell line. In this study, we have developed a conjugate of bombesin having very high affinity for the GRP-receptor holding an N-terminal fluorescent tag that might be useful in determining the diagnosis and disease progression of estrogen receptor positive (ER+) breast cancer. Targeting ER+ breast cancer cells *via* a targeting vector bearing a fluorescent label is a viable alternative to traditional radiolabeled conjugates of this general type.

The new Alexa Fluor 680-GGG-BBN(7-14)NH_2 conjugate (Figure 6) was conveniently synthesized by solid phase peptide synthesis of the parent BBN ligand followed by N-terminal conjugation of the active succinimidyl ester of the Alexa Fluor molecule (Ma et al., 2007). This conjugation technology provides a mechanism for appending large molecular weight molecules having inherent fluorescent properties to either the N-terminal primary amine or the epsilon primary amines of lysine-containing peptides or antibodies to produce stable conjugates for dynamic *in vivo* optical imaging. Less-reactive amidated C-termini, however, do not readily react with succinimidyl esters, making this a very selective conjugation method. In our hands, AF 680-GGG-BBN(7-14)NH_2 conjugate was stable at temperatures of -80 °C for periods extending 6 months. Other Alexa Fluor® 680 compounds of this general type designed and developed in our laboratory have demonstrated similar stability profiles.

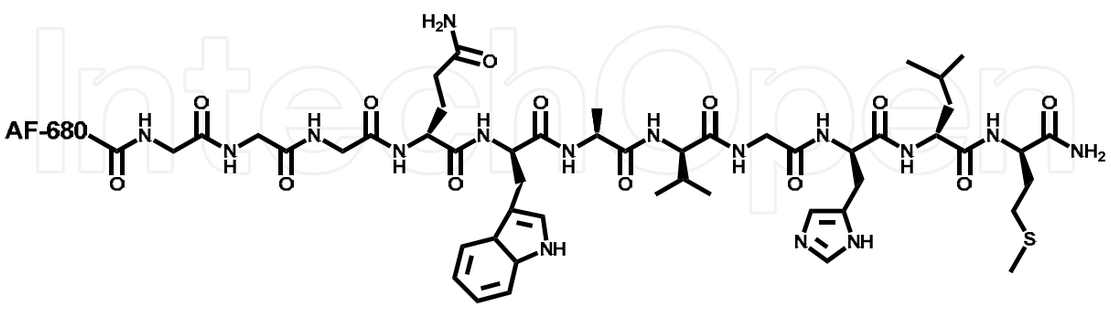

Fig. 6. AF 680-GGG-BBN(7-14)NH_2 conjugate.

In order to assess the binding affinity of the Alexa Fluor 680-GGG-BBN(7-14)NH_2 conjugate for the GRPr, *in vitro* competitive cell-binding assays were performed on T-47D breast cancer cells using ^{125}I-[Tyr^4]-BBN(7-14)NH_2 as the displacement radioligand. This new peptide conjugate demonstrated very high affinity for the GRPr in T-47D breast cancer cells, exhibiting an IC_{50} value of 7.7 ± 1.4 nM.

Figure 7 summarizes the results of studies to assess the degree of uptake, internalization, and blocking of the Alexa Fluor-GGG-BBN(7-14)NH_2 conjugate in T-47D breast cancer cells *via* confocal fluorescence microscopy. Assessment of the degree of AF 680-GGG-BBN(7-14)NH_2 conjugate associated with the cells after a 40 min incubation period was evaluated following a cell wash with pH 7.4 incubation media. Results of these studies clearly indicate the effectiveness of AF 680-GGG-BBN(7-14)NH_2 to specifically target the GRPr. To assess receptor-mediated internalization of AF 680-GGG-BBN(7-14)NH_2 conjugate, surface-bound conjugate was removed using pH 2.5 (0.2 M acetic acid and 0.5 M NaCl) buffer. After the acid wash, much of the conjugate remained internalized within the cells. *In vitro* blocking studies, in which high levels of BBN(1-14) were administered to the cells prior to the AF 680-GGG-BBN(7-14)NH_2 conjugate, reduced the uptake/retention in normal GRPr-expressing T-47D cells. This illustrates the high affinity and selectivity of this conjugate for GRPrs over-expressed on T-47D breast cancer cells. In fact, there is little or no indication of fluorescent signal associated with the cells following the blocking experiment.

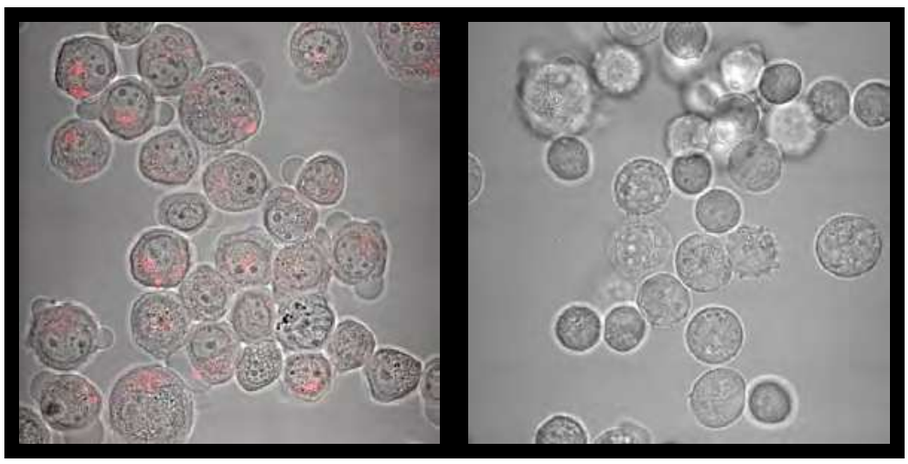

Fig. 7. Confocal fluorescence photomicrograph of internalized uptake of Alexa Fluor 680-GGG-BBN(7-14)NH_2 in human T-47D breast cancer cells (left). Confocal fluorescence photomicrograph of blocked uptake of Alexa Fluor 680-G-G-G-BBN(7-14)NH_2 in human T-47D breast cancer cells by wild-type BBN(1-14).

To assess the *in vivo* uptake of the Alexa Fluor conjugate, we have evaluated AF 680-GGG-BBN(7-14)NH_2 in rodents bearing human T-47D cancer cell xenografted tumors. In this study, dynamic optical imaging studies of T-47D breast cancer tumor xenografts in rodent models demonstrated the effectiveness of AF 680-GGG-BBN(7-14)NH_2 to specifically target GRPr-expressing cells *in vivo*. Montet and co-workers have demonstrated the effectiveness of fluorescent bombesin conjugates to effectively target implanted tumors of the pancreas (Montet et al., 2006). However, the effectiveness of imaging was only demonstrated using excised pancreatic/tumor tissue. Our more recent investigations have indicated specific uptake of conjugate in human tumor tissue (Figure 8a) in xenografted rodent models. Some degree of uptake was also observed in collateral tissue of the abdomen. This, however, is not entirely unexpected due to the hydrophobic nature of the high molecular weight targeting vector. Blocking investigations (Figure 8b), in which BBN(1-14) was used to saturate the GRPr prior to administration of AF 680-GGG-BBN(7-14)NH_2, showed little or no fluorescent signal associated with tumor tissue. To complement and verify the presence of GRPr-

expressing tumors, magnetic resonance imaging was performed (Figure 8c and 8d). These studies further demonstrate the high degree of selectivity and affinity of AF 680-GGG-BBN(7-14)NH_2 conjugate for the GRPr.

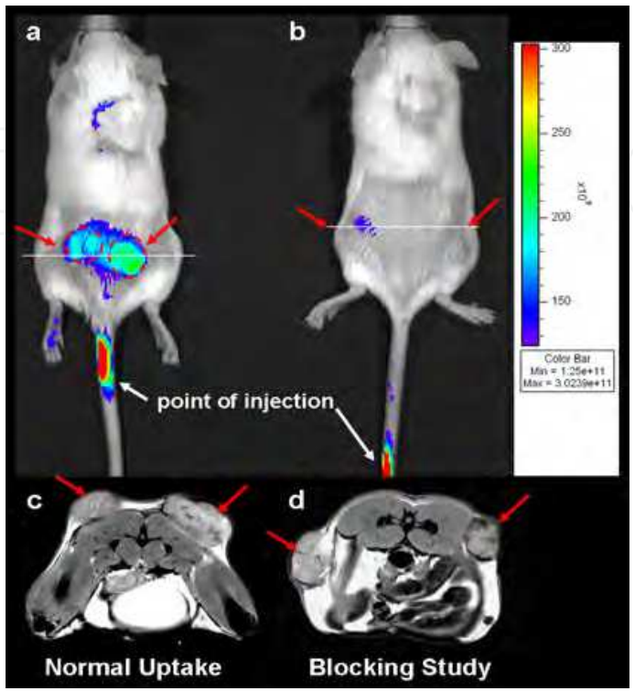

Fig. 8. *In vivo* uptake and blocking experiment of Alexa Fluor 680-GGG-BBN(7-14)NH_2 in SCID mice bearing human T-47D breast cancer cell xenografts. Xenogen fluorescence images of mice with (A) normal uptake and (B) blocking assay. Magnetic resonance images of cross sections through tumors for (C) normal uptake and (D) blocking assay.

7. Conclusion

The clinical successes of Octreoscan® have paved the way for exploration and radiolabeling of biologically-active peptides for targeted molecular imaging and peptide receptor scintigraphy of receptors that are highly expressed on specific human tumors. This book chapter has focused primarily upon those peptides that are potentially useful for molecular imaging of human breast cancer. Specifically, our research investigations have focused primarily upon targeting GRPrs with truncated analogues of BBN peptide, as these receptors tend to be expressed in very high numbers on the surface of breast cancer cells. However, there are other cancer types that also express regulatory peptide receptors in very high numbers, making possible early diagnosis and staging of primary and metastatic disease for these cancers as well. More importantly, continued research efforts toward development of thermodynamically stable, kinetically inert radiolabeled peptides for specific targeting of receptors that are highly expressed on the surfaces of human cancer cells creates the opportunity to use peptide receptor targeted radiotherapy as a highly selective treatment strategy for tumor targeting of breast cancer and many others, or as a mechanism for this treatment strategy to complement traditional, clinically-useful chemotherapeutic regimens of treatment.

8. Future work

Until now, the molecular basis for GRPr-targeted diagnosis or therapy of receptor-positive neoplastic disease has primarily focused upon targeting receptor over-expression using radiolabeled agonist ligands with inherent internalizing capability. However, recent reports by Nock et al., show compelling evidence that radiopharmaceutical design and development based upon antagonist-type ligand frameworks bear reexamination (Nock et al., 2003 and 2005). Antagonist ligands are presumably not internalized, and therefore are not expected to residualize as effectively in tumor tissue when compared to agonist-based ligand frameworks. Studies using ^{99m}Tc-Demobesin1 ([^{99m}Tc-$N_4^{0\text{-}1}$,bzlg^{0},D-Phe^{6},Leu-NHEt^{13},des-Met^{14}]BBN(6-14)) demonstrated very high affinity and selectivity for the GRPR with pronounced accumulation and retention of radioactivity in human tumor xenografts in rodents (Nock et al., 2003 and 2005). In addition, Maecke and co-workers have begun investigating another antagonist-like targeting vector, [DOTA-4-amino-1-carboxymethyl-piperidine-D-Phe-Gln-Trp-Ala-Val-Gly-His-Sta-Leu-NH_2], having high selectivity for the GRPr (Mansi et al., 2009 and 2011). Therefore, selective targeting of specific receptor subtypes expressed on the surfaces of primary or metastatic breast cancer tissues with new and improved radiolabeled antagonists might provide a new avenue for earlier diagnosis and staging of patients presenting with disease.

In addition, we should point out that discussions herein have only considered monomeric peptide targeting vectors for molecular imaging of breast cancer tissue. It is important to note that the clinical utility of monomeric radiolabeled peptides can be limited by a number of factors including receptor density, binding affinity, and pharmacokinetics. For example, high-quality, high tumor-to-background PET or SPECT images require a high degree of receptor expression on tumor cells as compared to normal, collateral tissue. For these reasons, multimeric or multivalent peptide probes have recently become a new avenue for diagnostic molecular imaging tumors expressing either singly- or multi-targetable receptors. Continued design and development of multimeric or multivalent peptides capable of targeting multiple receptor subtypes highly expressed on human cancers could do much to improve image resolution and contrast, all but eliminating the high false-positive rates and non-target uptake that oftentimes limits some of the clinically-approved radiopharmaceuticals from widespread usage for diagnosis of malignant tissues.

9. Acknowledgment

This material is the result of work supported with resources and the use of facilities at the Harry S. Truman Memorial Veterans' Hospital and the University of Missouri School of Medicine. This work was funded in part by grants from the National Institutes of Health and the United States Department of Veterans' Affairs VA Merit Award.

10. References

American Cancer Society. *Cancer Facts and Figures 2010, Detailed Guide: Breast Cancer.* The American Cancer Society, Atlanta: 2010. Available at www.cancer.org/acs/groups/content/@epidemiologysurveilance/documents/document/acspc-026210.pdf

Abd-Elgaliel WR, Gallazzi F, Garrison JC, et al. (2008). Design, Synthesis, and Biological Evaluation of an Antagonist-Bombesin Analogue as Targeting Vector. *Bioconj. Chem.,* Vol. 19: pp. 2040-2048.

Alberto R, Ortner K, Wheatley N, et al. (2001). Synthesis and properties of boranocarbonate: a convenient in situ CO source for the aqueous preparation of $[^{99m}Tc(OH_2)_3(CO)_3]^+$. *J. Am. Chem. Soc.,* Vol. 123, pp. 3135-3136.

Alberto R, Schibli R, Egli A, et al. (1998). A novel organometallic aqua complex of technetium for the labeling of biomolecules: synthesis of $[^{99m}Tc(OH_2)_3(CO)_3]^+$ from $[^{99m}TcO_4]^-$ in aqueous solution and its reaction with a bifunctional ligand. *J. Am. Chem. Soc.,* Vol. 120, pp. 7987-7988.

Aliaga A, Rousseau JA, Ouellette R, et al. (2004). Breast cancer models to study the expression of estrogen receptors with small animal PET imaging. *Nucl. Med. Biol.*, Vol. 31, pp. 761-770.

Anderson CJ & Welch MJ. (1999). Radiometal-Labeled Agents (Non-Technetium) for Diagnostic Imaging. *Chem. Rev.,* Vol. 99, pp. 2219-2234.

Bajc M, Ingvar C. & Palmer J. (1996). Dynamic Indium-111-Pentetreotide Scintigraphy in Breast Cancer. *J. Nuc. Med.,* Vol. 37, pp. 622-626.

Berghammer P, Obwegeser R, & Sinzinger H. (2001). Nuclear medicine and breast cancer: a review of current strategies and novel therapies. *The Breast,* Vol. 10, pp. 184-197.

Biddlecombe GB, Rogers BE, de Visser M, et al. (2007) Molecular imaging of GRP receptor positive tumors in mice using ^{64}Cu- and ^{86}Y-DOTA-(Pro1,Tyr4)-BBN(1-14). *Bioconj. Chem.,* Vol. 18, pp. 724-730.

Biersack HJ & Freeman LM (eds). (2007). *Clinical Nuclear Medicine,* Springer, New York.

Blok D, Feitsma RIJ, Vermeij P, et al. (1999). Peptide radiopharmaceuticals in nuclear medicine. *Eur. J. Nucl. Med.,* Vol. 26, pp. 1511-1519.

Blower PJ, Lewis JS, & Zweit J. (1996). Copper radionuclides and radiopharmaceuticals in nuclear medicine. *Nucl. Med. Biol.,* Vol. 23, pp. 957-980.

Coy DH, Heinz-Erian P, Jiang NY, et al. (1988). Probing peptide backbone function in bombesin. A reduced peptide bond analogue with potent and specific receptor antagonist activity. *Bioconj. Chem.*, Vol. 263, pp. 5056-5060.

Cuttitta F, Carney DN, Mulshine J, et al. (1985). BBN-like peptides can function as autocrine growth factors in human small-cell lung cancer. *Nature,* Vol. 316, pp. 823-825.

Di Bartolo NM, Sargeson AM, Donlevy TM, et al. (2001). Synthesis of a new cage ligand, SarAr, and its complexation with selected transition metal ions for potential use in radioimaging. *J Chem. Soc., Dalton Trans*, pp. 2303-2309.

Di Bartolo NM, Sargeson AM & Smith SV. (2006). New ^{64}Cu PET imaging agents for personalized medicine and drug development using the hexa-aza cage, SarAr. *Org. Biomol. Chem.,* Vol. 4, pp. 3350-3357.

Engel LW & Young NA. (1978). Human breast carcinoma cells in continuous culture: a review. *Can. Res.*, Vol. 38, pp. 4327-4339.

Fischman AJ, Babich JW, & Strauss HW. (1993). A Ticket to Ride: Peptide Radiopharmaceuticals. *J. Nucl. Med.,* Vol. 34, pp. 2253-2263.

Garrison JC, Rold TL, Sieckman GL, et al. (2007). *In vivo* evaluation and small-animal PET/CT of a prostate cancer mouse model using ^{64}Cu BBN analogs: side-by-side comparison of the CB-TE2A and DOTA chelation systems. *J. Nucl. Med.,* Vol. 48, pp. 1327-1337.

Gasser G, Tjioe L, Graham B, et al. (2008). Synthesis, copper(II) complexation, ^{64}Cu-labeling, and bioconjugation of a new bis(2-pyridylmethyl) derivative of 1,4,7-triazacyclononane. *Bioconj. Chem.,* Vol. 19, pp. 719-730.

Geraldes CFGC, Marques MP, de Castro B, et al. (2000). Study of copper(II) polyazamacrocyclic complexes by electronic absorption spectrophotometry and EPR spectroscopy. *Eur. J. Inorg. Chem.*, pp. 559-565.

Giacchetti S, Gauville C, De Cremoux P, et al. (1990). Characterization, In Some Human Breast Cancer Cell Lines, of Gastrin-Releasing Peptide-Like Receptors Which are Absent in Normal Breast Epithelial Cells. *Int. J. Can.,* Vol. 46, pp. 293-298.

Giblin MF, Gali H, Sieckman GL, et al. (2006). *In vitro* and *in vivo* evaluation of ^{111}In-labeled E. coli heat-stable enterotoxin analogs for specific targeting of human breast cancers. *Breast Can. Res. Treat.*, Vol. 98, pp. 7-15.

Gopalan D, Bomanji JB, Costa DC, et al. (2002). Nuclear Medicine in Primary Breast Cancer Imaging. *Clin. Radiol.,* Vol. 57, pp. 565-574.

Gugger M & Reubi JC. (1999). Gastrin-Releasing Peptide Receptors in Non-Neoplastic and Neoplastic Human Breast. *Am. J. Path.,* Vol. 155, pp. 2067-2076.

Guojun W, Wei G, Kedong O, et al. (2008). A novel vaccine targeting pastrin-releasing peptide: efficient inhibition of breast cancer growth *in vivo*. *Endocrine-Related Cancer*, Vol. 15, pp. 149-159.

Hoffman TJ, Quinn TP, & Volkert WA. (2001). Radiometallated receptor-avid peptide conjugates for specific *in vivo* targeting of cancer cells. *Nucl. Med. Biol.,* Vol. 28, pp. 527-539.

Jones CJ and Thornback JR. (2007). *Medical Applications of Coordination Chemistry,* RSC Publishing, Cambridge, UK.

Kaida H, Ishibashi M, Fujii T, et al. (2008). Improved detection of breast cancer on FDG-PET cancer screening using breast positioning device. *Ann. Nucl. Med.*, Vol. 22, pp. 95-101.

Katzenellenbogen JA, Coleman RE, Hawkins RA, et al. (1995). Tumor Receptor Imaging: Proceedings of the National Cancer Institute Workshop, Review of Current Work, and Prospective for Further Investigations. *Clin. Can. Res.,* Vol. 1, 921-932.

Knigge U, Holst JJ, Knuhtsen S, et al. (1984). Gastrin-Releasing Peptide: Pharmacokinetics and Effects on Gastroentero-Pancreatic Hormones and Gastric Secretion in Normal Men. *J. Clin. Endocrin. Metab.,* Vol. 59, pp. 310-315.

Koglin N & Beck-Sickinger AG. (2004). Novel modified and radiolabelled neuropeptide Y analogues to study Y-receptor subtypes. *Neuropeptides,* Vol. 38, pp. 153-161.

Krause W. (ed.) (2002). *Contrast Agents II: Optical, Ultrasound, X-Ray, and Radiopharmaceutical Imaging,* Springer, New York.

Kukis DL, Li M, & Meares CF. (1993). Selectivity of antibody-chelate conjuates for binding copper in the presence of competing metals. *Inorg. Chem.*, Vol. 32, pp. 3981-3982.

Kwon S, Ke S, Houston JP, et al. (2005). Imaging dose-dependent pharmacokinetics of an RGD-fluorescent dye conjugate targeted to avb3 receptor expressed in Kaposi's sarcoma. *Mol. Imaging*, Vol. 4, No. 2, pp. 75-87.

Lacroix M & Leclercq G. (2004). Relevance of breast cancer cell lines as models for breast tumors: an update. *Breast Can. Res. Treat.*, Vol. 83, pp. 249-289.

Lixin M, Yu P, Veerendra B, et al. (2007). *In vitro* and *In vivo* Evaluation of AF 680-BBN[7-14]NH_2 Peptide Conjugate, a High-Affinity Fluorescent Probe with High Selectivity for the GRP Receptor. *Mol. Imaging,* Vol. 6, pp. 171-180.

Maina T, Nock BA, Zhang H, et al. (2005). Species differences of bombesin analog interactions with GRP-R define the choice of animal models in the development of GRP-R-targeting drugs. *J. Nucl. Med.*, Vol. 46, pp. 823-830.

Mansi, R., Wang X, Forrer F et al. (2009). Evaluation of a 1,4,7,10-tetraazacyclododecane-1,4,7,10-tetraacetic acid-conjugated BBN-based radioantagonist for the labeling with single-photon emission computed tomography, positron emission tomography, and therapeutic radionuclides. *Clin. Can. Res.*, Vol. 15, No. 16, pp. 5240-5249.

Mansi, R., Wang X, Forrer F, et al. (2011). Development of a potent DOTA-conjugated BBN antagonist for targeting GRPr-positive tumours. *Eur. J. Nucl. Med. Mol. Imag.*, Vol. 38, No. 1, pp. 97-107.

Monstein HJ, Grahn N, Truedsson M, et al. (2006). Progastrin-releasing peptide and gastrin-releasing peptide receptor mRNA expression in non-tumor tissues of the human gastrointestinal tract. *World J. Gastroenterol.*, Vol. 12, pp. 2574-2578.

Montet X, Weissleder R & Josephson L (2006). Imaging pancreatic cancer with a peptide-nanoparticle conjugate targeted to normal pancreas. *Bioconj. Chem.*, Vol. 27, pp. 905-911.

Moody TW & Gozes I. (2007). Vasoactive Intestinal Peptide Receptors: A Molecular Target in Breast and Lung Cancer. *Cur. Pharmaceutical Des.,* Vol. 13, pp. 1099-1104.

Moody TW, Pert CB, Gazdar AF, et al. (1981). High levels of intracellular BBN characterize human small cell lung carcinoma. *Science,* Vol. 214, pp. 1246-1248.

Nass SJ, Henderson IC, & Lashof JC (eds). (2001). *Mammography and Beyond: Developing Technologies for the Early Detection of Breast Cancer.* Natl. Acad. Press, Washington.

Nijsen JFW, Krijer GC, & van het Schip AD. (2007). The bright future of radionuclides for cancer therapy. *Anti Canc. Agents Med. Chem.*, Vol. 7, pp. 271-290.

Nock B, Nikolopoulou A, Chiotellis E, et al. (2003). [^{99m}Tc] Demobesin 1, a novel potent bombesin analogue for GRPr-targeted tumour imaging. *Eur. J. Nucl. Med. Mol. Imag.,* Vol. 30, pp. 247-258.

Nock B, Nikolopoulou A, Galanis A, et al. (2005). Potent bombesin-like peptides for GRP-receptor targeting of tumors with ^{99m}Tc: A preclinical study. *J. Med. Chem.*, Vol. 48, No. 1, pp. 100-110.

Olsen, O & Gotzsche PC. (2001). Cochrane Review on Screening for Breast Cancer with Mammography. *Lancet.* Vol. 358, pp. 1340-1342.

Parry JJ, Andrews R, & Rogers BE. (2007). MicroPET imaging of breast cancer using radiolabeled bombesin analogs targeting the gastrin-releasing peptide receptor. *Breast Can. Res. Treat.*, Vol. 101, pp. 175-183.

Pippin CG, Kumar K, Mirzadeh S, et al. (1991). Kinetics of the isotopic exchange between copper(II) and copper(II) 1,4,7-triazacyclononane-*N*,*N*′,*N*′′ triacetate. *J. Labeled Comp. Rad.*, Vol. 30, p. 221.

Pisano ED, Gatsonis C, Hendrick E, et al. (2005). Diagnostic performance of digital versus film mammography for breast-cancer screening. *New Engl. J. Med.*, Vol. 353, pp. 1773-1783.

Pomper MG & Gelovani JG (eds). (2008). *Molecular Imaging in Oncology.* Informa Healthcare, New York.

Prasad NS, & Houserkova D. (2007). The roles of various modalities in breast imaging. *Biomed Pap Fac Univ Palacky Olomouc Czech Republic*, Vol. 151, pp. 209-218.

Prasanphanich AF, Lane SR, Figueroa SD, et al. (2007). The effects of linking substituents on the *in vivo* behavior of site-directed, peptide-based, diagnostic radiopharmaceuticals. *In Vivo*, Vol. 21, pp. 1-16.

Prasanphanich AF, Nanda PK, Rold TL, et al. (2007). [^{64}Cu-NO2A-8-Aoc-BBN(7-14)NH_2] targeting vector for PET imaging of gastrin-releasing peptide receptor-expressing tissues. *Proc. Natl. Acad. Sci. USA*, Vol. 104, pp. 12462-12467.

Prasanphanich AF, Retzloff L, Lane SR, et al. (2009). *In vitro* and *in vivo* analysis of [^{64}Cu-NO2A-8-Aoc-BBN(7-14)NH_2]: a site-directed radiopharmaceutical for positron emission tomography imaging of T-47D human breast cancer tumors. *Nucl. Med. and Biol.,* Vol. 36, pp. 171-181.

Pu Y, Wang WB, Tang GC, et al. (2005). Spectral polarization imaging of human prostate cancer tissue using a near-infrared receptor-targeted contrast agent. *Tech. Canc. Res. Treat*. Vol. 4, No. 4, pp. 429-436.

Retzloff, LB, Heinzke, L, Figureoa, SD et al. (2010). Evaluation of [^{99m}Tc-$(CO)_3$-X-Y-Bombesin(7-14)NH_2] Conjugates for Targeting Gastrin-releasing Peptide Receptors Over-expressed on Breast Carcinoma. *Antican. Res.*, Vol. 30, pp.19-30.

Reubi, JC. (2008). Peptide Receptors as Molecular Targets for Cancer Diagnosis and Therapy. *Endocrine Rev.,* Vol. 124, pp. 389-427.

Rosen ST, Blake MA, & Kalra MK (eds). (2008). *Cancer Treatment and Research, Volume 143: Imaging in Oncology.* Springer, New York.

Schibli R & Schubiger PA. (2002). Current use and future potential of organometallic radiopharmaceuticals. *Eur. J. Nucl. Med.,* Vol. 29, pp. 1529-1542.

Scopinaro F, Varvarigou AD, Ussof W, et al. (2002). Technetium Labeled Bombesin-like Peptide: Preliminary Report on Breast Cancer Uptake in Patients. *Canc. Biother. Rad.,* Vol. 17, pp. 327-335.

Signore A, Annovazzi A, Chianelli M, et al. (2001). Peptide radiopharmaceuticals for diagnosis and therapy. *Eur. J. Nucl. Med.,* Vol. 28, pp. 1555-1565.

Smith CJ, Gali H, Sieckman GL, et al. (2003). Radiochemical Investigations of ^{99m}Tc-N_3S-X-BBN[7-14]NH_2: An *in vitro/in vivo* Structure-Activity Relationship Study Where X = 0-, 3-, 5-, 8-, and 11-Carbon Tethering Moieties. *Bioconj.Chem.,* Vol. 14, pp. 93-102.

Smith CJ, Volkert WA, & Hoffman TJ. (2003). Gastrin releasing peptide receptor targeted radiopharmaceuticals: A concise update. *Nucl. Med. Biol.,* Vol. 30, pp. 861-868.

Smith CJ, Volkert WA, & Hoffman TJ. (2005). Radiolabeled peptide conjugates for targeting of the BBN receptor superfamily subtypes. *Nucl. Med. Biol.,* Vol. 32, pp. 733-740.

Soluri A, Scopinaro F, de Vincentis G, et al. (2003). ^{99m}Tc [13Leu] bombesin and a new gamma camera, the probe, are able to guide mammotome breast biopsy. *Antican. Res.*, Vol. 23, pp. 2139-2142.

Sprague JE, Peng Y, Fiamengo AL, et al. (2007). Synthesis, characterization and *in vivo* studies of Cu(II)-64-labeled cross-bridged tetraazamacrocycle-amide complexes as models of peptide conjugate Imaging Agents. *J. Med. Chem.*, Vol. 50, pp. 2527-2535.

Stigbrand T, Carlsson J, & Adams GP (eds). (2008). *Targeted Radionuclide Tumor Therapy: Biological Aspects.* Springer, New York.

Sun YG, & Chen ZF. (2007). A gastrin-releasing peptide receptor mediates the itch sensation in the spinal cord. *Nature*, Vol. 488, pp. 700-703.

Thakur ML, Aruva MR, Gariepy J, et al. (2004). PET Imaging of Oncogene Over-expression Using: ^{64}Cu-Vasoactive Intestinal Peptide (VIP) Analog: Comparison with ^{99m}Tc-VIP Analog. *J. Nucl. Med.,* Vol. 45, pp. 1381-1389.

Van de Wiele C, Dumont F, Broecke RV, et al. (2000). Technetium-99m RP527, a GRP analogue for visualisation of GRPr-expressing malignancies: a feasibility study. *Eur. J. Nucl. Med.,* Vol. 27, pp. 1694-1699.

van der Merwe MJ, Boeyens JCA, & Hancock RD. (1985). Crystallographic and thermodynamic study of metal ion size selectivity in the ligand 1,4,7-triazacyclononane-*N*,*N*′,*N*′′-triacetate. *Inorg. Chem.*, Vol. 24, pp. 1208-1213.

Varvarigou A, Bouziotis P, Zikos C, et al. (2004). Gastrin-Releasing Peptide (GRP) Analogues for Cancer Imaging. *Canc. Biother. Rad.,* Vol. 19, pp. 219-229.

Voss SD, Smith SV, Di Bartolo NM, et al. (2007). Positron emission tomography (PET) imaging of neuroblastoma and melanoma with ^{64}Cu-SarAr immunoconjugates. *Proc. Natl. Acad. Sci. USA*, Vol. 104, pp. 17489-17493.

Wadas TJ, Wong EH, Weisman GR, et al. (2007). Copper chelation chemistry and its role in copper radiopharmaceuticals. *Cur. Pharmaceutical Des.*, Vol. 13, pp. 3-16.

Wang F, Wang Z, Wu J, et al. (2008). The role of technetium-99m-labeled octreotide acetate scintigraphy in suspected breast cancer and correlates with expression of SSTR. *Nucl. Med. Biol.,* Vol. 35, pp. 665-671.

Weiner RE, & Thakur ML. (2005). Radiolabeled peptides in oncology. *Biodrugs*, Vol. 19, pp. 145-163.

Weissleder R, & Ntziachristos, V (2003). Shedding light onto live molecular targets. *Nat. Med.*, Vol. 9, pp. 123-128.

Wieghardt K, Bossek U, Chaudhuri P, et al. (1982). 1,4,7-Triazacyclononane-*N*,*N*′,*N*′′-triacetate (TCTA), a hexadentate ligand for divalent and trivalent metal ions. Crystal structures of [Cr^{III}(TCTA)], [Fe^{III}(TCTA)], and Na[Cu^{II}(TCTA)]•2NaBr•8H_2O. *Inorg. Chem.,* Vol. 21, pp. 4308-4314.

Young SH, & Rozengurt E (2006). Quantum dots conjugated to bombesin or angiotensin II label the cognate G protein-coupled receptor in living cells. *Am. J. Physiol. Cell Physiol.*, Vol. 290, No. 3, pp. 728-732.

Zacharakis, G, Ripoll, J, & Ntziachristos, V (2005). Fluorescent protein tomography scanner for small animal imaging. *IEEE Trans. Med. Imag.,* Vol. 24, pp. 878-885.

Zhang H, Chen J, Waldherr C, et al. (2004). Synthesis and Evaluation of Bombesin Derivatives on the Basis of Pan-Bombesin Peptides Labeled with Indium-111, Lutetium-177, and Yttrium-90 for Targeting Bombesin Receptor-Expressing Tumors. *Can. Res.,* Vol. 64, pp. 6707-6715.

Zhou J, Chen J, Mokotoff M, et al. (2003). Bombesin/gastrin-releasing peptide receptor: a potent target for antibody-mediated therapy of small cell lung cancer. *Clin. Can. Res.,* Vol. 9, pp. 4953-4960.

Zwanziger D, Khan IU, Neundorf I, et al. (2008). Novel Chemically Modified Analogues of Neuropeptide Y for Tumor Targeting. *Bioconj. Chem.,* Vol. 19, pp. 1430-1438.

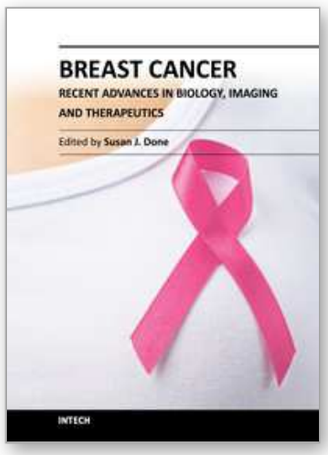

Breast Cancer - Recent Advances in Biology, Imaging and Therapeutics

Edited by Dr. Susan Done

ISBN 978-953-307-730-7
Hard cover, 428 pages
Publisher InTech
Published online 14, December, 2011
Published in print edition December, 2011

In recent years it has become clear that breast cancer is not a single disease but rather that the term encompasses a number of molecularly distinct tumors arising from the epithelial cells of the breast. There is an urgent need to better understand these distinct subtypes and develop tailored diagnostic approaches and treatments appropriate to each. This book considers breast cancer from many novel and exciting perspectives. New insights into the basic biology of breast cancer are discussed together with high throughput approaches to molecular profiling. Innovative strategies for diagnosis and imaging are presented as well as emerging perspectives on breast cancer treatment. Each of the topics in this volume is addressed by respected experts in their fields and it is hoped that readers will be stimulated and challenged by the contents.

How to reference

In order to correctly reference this scholarly work, feel free to copy and paste the following:

Andrew B. Jackson, Lauren B. Retzloff, Prasant K. Nanda and C. Jeffrey Smith (2011). Molecular Imaging of Breast Cancer Tissue via Site-Directed Radiopharmaceuticals, Breast Cancer - Recent Advances in Biology, Imaging and Therapeutics, Dr. Susan Done (Ed.), ISBN: 978-953-307-730-7, InTech, Available from: http://www.intechopen.com/books/breast-cancer-recent-advances-in-biology-imaging-and-therapeutics/molecular-imaging-of-breast-cancer-tissue-via-site-directed-radiopharmaceuticals

INTECH
open science | open minds

InTech Europe
University Campus STeP Ri
Slavka Krautzeka 83/A
51000 Rijeka, Croatia
Phone: +385 (51) 770 447
Fax: +385 (51) 686 166
www.intechopen.com

InTech China
Unit 405, Office Block, Hotel Equatorial Shanghai
No.65, Yan An Road (West), Shanghai, 200040, China
中国上海市延安西路65号上海国际贵都大饭店办公楼405单元
Phone: +86-21-62489820
Fax: +86-21-62489821

© 2011 The Author(s). Licensee IntechOpen. This is an open access article distributed under the terms of the Creative Commons Attribution 3.0 License, which permits unrestricted use, distribution, and reproduction in any medium, provided the original work is properly cited.

IntechOpen

IntechOpen